Dark respiration modulates photosynthetic carbon yield in cyanobacteria

Ningdong Xie[1], Chetna Sharma[1], Katy Rusche[2], Xin Wang[1]*

[1]Department of Microbiology and Cell Science, Institute of Food and Agricultural Sciences, University of Florida, Gainesville FL 32611

[2]Department of Microbiology, Miami University, Oxford OH 45056

*Correspondence: wangx3@ufl.edu

Abstract

Cyanobacteria contribute to roughly a quarter of global net carbon fixation. During diel light/dark growth, dark respiration significantly lowers the overall photosynthetic carbon yield in cyanobacteria and other phototrophs. Currently, it is unclear how photosynthetic organisms allocate carbon resources at night for optimal dark survival. Here we show in the cyanobacterium *Synechococcus elongatus* PCC 7942 that phosphoketolase and 2-keto-3-deoxy-6-phosphogluconate (KDPG) aldolase are orchestrated in an integrative respiratory network in the dark to best allocate carbon resource for amino acid synthesis and preparation for photosynthesis reinitiation upon photoinduction. We further show that the Entner-Doudoroff (ED) pathway is incomplete in *S. elongatus* with the KDPG aldolase participating in dark respiration through an alternative decarboxylation activity. Optimization of dark respiration thus represents a unique strategy to enhance photosynthetic carbon yield in cyanobacteria and other photosynthetic organisms.

Introduction

Cyanobacteria account for approximately a quarter of global net primary production[1,2]. In their natural environment, cyanobacteria and many other photosynthetic organisms experience diel light/dark growth cycles. During the day, photon energy is converted to chemical energy to support growth and synthesize storage polymers. At night, cellular respiration breaks down these storage compounds to support cell maintenance in the dark[3]. Respiration in the dark thus contributes to significant carbon loss in photosynthetic organisms. In plants, respiration alone can lead to as much as 15-30% of carbon loss, significantly lowering the overall photosynthetic carbon yield[4]. Optimization of respiratory metabolism thus could minimize carbon loss and enhance the overall photosynthetic carbon yield[5,6]. However, studies on respiration and its relations to photosynthesis are relatively sparse. One recent study showed that some of the most prevalent phototrophic microbial lineages in the surface ocean have several fold higher respiration rates at night than the daytime[7].

In cyanobacteria, glycogen is the main energy storage polymer synthesized under light. Glycogen degradation in the dark supplies simple sugars to the oxidative pentose phosphate (OPP) pathway, generating NADPH for energy production through the electron transport chain[8,9]. On the other hand, NADPH also serves as cofactors for many detoxification enzymes to clean up reactive oxygen species (ROS) accumulated in the light[10]. Although it is well known about this general scheme of cell maintenance in the dark, the details of cellular metabolic state and energy conservation strategy in the dark are far less clear. For instance, since little DNA replication is occurring at night[11,12], the metabolic destination of C_5 sugars derived from the OPP pathway is intriguing to understand.

When cyanobacteria enter darkness, enzymes for carbon fixation become inactivated[13], switching cell metabolism to catabolic reactions. In *Synechococcus elongatus* PCC 7942 (hereafter *S. elongatus*), a relatively stable metabolic profile is observed during the first few hours of the night, in contrast to a more drastic metabolic changes in the circadian transcription factor mutant (Δ*rpaA*)[10], suggesting a tight circadian regulation on dark respiration. After dark respiration,

several intermediates in the Calvin-Benson-Bassham (CBB) cycle become limited, requiring replenishment for the optimal reinitiation of the CBB cycle reactions upon light exposure[14]. Previously, we observed that unlike other CBB cycle intermediates, 3-phosphoglycerate (3PG) accumulates even after darkness and is maintained at a relatively high level during the photosynthesis initiation period[14]. This accumulation is not observed in the glycogen synthesis mutant (Δ*glgC*)[14], indicating the origin of 3PG from glycogen degradation in the dark. Through a non-steady-state metabolic flux analysis, a recent study showed that 3PG accumulated in the dark could serve as the precursor for carbon regeneration reactions in the CBB cycle during photoinduction[15]. Carbon fixation is delayed until the starting substrate ribulose-1,5-bisphosphate (RuBP) is synthesized through carbon regeneration reactions in the CBB cycle. Moreover, 3PG accumulated in the dark also serves as the electron acceptor to quench energy from light reactions upon photoinduction. This energy quenching role of 3PG is thus crucial for protecting photosystems from photodamage.

Dissecting the respiratory network in the dark is central for improving the overall photosynthetic carbon yield in cyanobacteria and other phototrophs. Currently, the metabolic mechanisms through which cyanobacteria allocate carbon and energy resources for efficient cell maintenance in the dark, and the strategies employed to maximize photosynthetic carbon yield during diel light/dark cycles, remain unclear. Here we show that the Entner-Doudoroff (ED) pathway is incomplete in *S. elongatus*, with the key enzyme 2-keto-3-deoxy-6-phosphogluconate (KDPG) aldolase participating in respiration through an alternative decarboxylation activity. Furthermore, we show that cyanobacteria form an integrative respiratory network, coupling the OPP pathway, phosphoketolase metabolism, the Embden-Meyerhof-Parnas (EMP) pathway, and the decarboxylation activity of KDPG aldolase, to ensure the optimal carbon allocation for cell maintenance and photosynthesis preparation.

Results

Glycogen degradation occurs early in the dark to replenish key intermediate pools

Glycogen metabolism is crucial for the fitness of cyanobacteria under diel light/dark growth[16]. We showed previously that *S. elongatus* glycogen synthesis mutant (Δ*glgC*) accumulated significantly less biomass than the wild type under 8h/16h light/dark growth cycles[14]. To better understand how growth is affected by different light/dark periods, we grew wild type and the Δ*glgC* mutant in three diel cycles that resemble light/dark lengths in the natural environment, i.e., 10h/14h, 12h/12h, and 14h/10h light/dark cycles. Under all three growth cycles, the Δ*glgC* mutant accumulated less final biomass compared to the wild type (Fig. 1a), suggesting glycogen synthesis as an important carbon and energy reservoir to enhance total photosynthetic carbon yield under diel growth.

To examine how glycogen levels change in the dark, the wild type and Δ*glgC* mutant were shifted to dark after continuous growth in the light to late log phase. No glycogen was detected in the Δ*glgC* mutant, consistent with the inability of this strain to synthesize glycogen (Fig. 1b). By contrast, the glycogen synthesized in wild type under light was reduced twofold in abundance during the initial six hours of darkness and remained at constant levels for the duration of the dark period (Fig. 1b). Based on our previous study, 3PG is more abundant at the end of the dark period in wild type than Δ*glgC* cells grown in 8h/16h light/dark cycles[14], suggesting that 3PG must be replenished through glycogen degradation during dark respiration. 3PG is a central metabolic intermediate for amino acid synthesis in the dark, and important for carbon fixation reactions upon light exposure[15]. Without glycogen storage, the depletion of 3PG may further disrupt cell metabolism and lead to a higher maintenance cost in the dark.

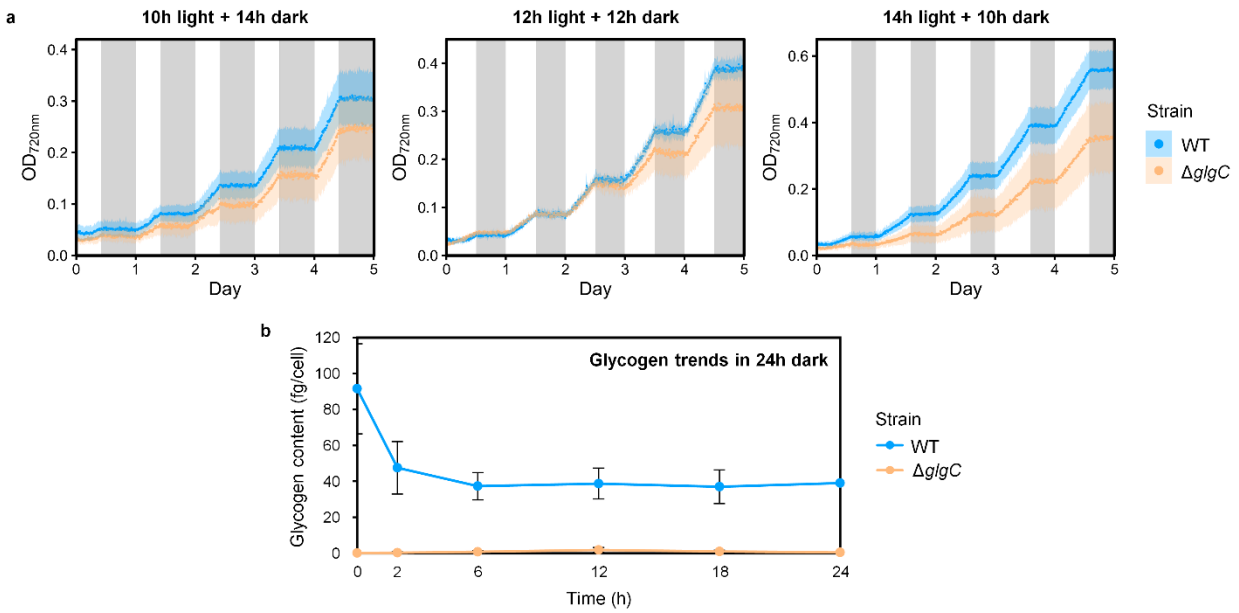

Figure 1. Glycogen degradation primarily occurs early in the dark. a, Diel growth of *S. elongatus* wild type (WT) and the glycogen synthesis mutant (Δ*glgC*) during the 10h/14h, 12h/12h, and 14h/10h light/dark cycles (100 μmol/m^2/s light intensity during the light phase). Dotted line and shade represent the OD_{720nm} mean and standard deviation, respectively. Grey shading represents the dark period of diel cycles. The terminal OD_{720nm} of WT is significantly higher ($p < 0.05$) than that of Δ*glgC* under the 14h/10h light/dark cycle. **b,** Temporal change of the glycogen content in WT and Δ*glgC* during a 24-hour dark period following a continuous growth in the light to late log phase. Circle and error bar resent the mean and standard deviation, respectively.

Phosphoketolase and KDPG aldolase contribute to optimal photosynthetic carbon yield under diel growth

In the dark, simple sugars from glycogen degradation are mainly routed to the OPP pathway for energy generation through respiration[8]. However, the process by which C_5 carbons from the OPP pathway will be further catabolized remains unclear. To illustrate the potential involvement of other respiratory pathways in the dark, we constructed mutants of the EMP, phosphoketolase, and ED pathways by deleting genes for the phosphofructokinase (Δ*pfk*), the phosphoketolase (Δ*pkt*), and the KDPG aldolase (Δ*eda*), respectively (Supplementary Fig. 1 and Supplementary

Table 1). These mutants were examined for growth under 10h/14h light/dark cycles to maximize the impact of dark respiration. The Δ*pfk* mutant showed similar growth to the wild type, suggesting a neglectable role of the upstream EMP pathway in supporting a robust diel growth (Fig. 2a). In contrast, the Δ*pkt* and Δ*eda* single and double mutants accumulated less biomass than the wild type under these diel growth conditions (Fig. 2b). By comparison, the Δ*pkt* mutant grew similarly to the wild type under continuous light (Fig. 2c). The Δ*eda* mutant also showed similar biomass accumulation to the wild type under continuous light but had a slight bleaching phenotype (Fig. 2d and Supplementary Fig. 2). These above results suggest that phosphoketolase and KDPG aldolase may optimize the carbon budget used in cell maintenance in the dark. Compared to the *S. elongatus* wild type, the Δ*pkt* and Δ*eda* mutants likely have disrupted intermediate pools and higher carbon loss that led to lower final biomass yield under diel light/dark growth cycles.

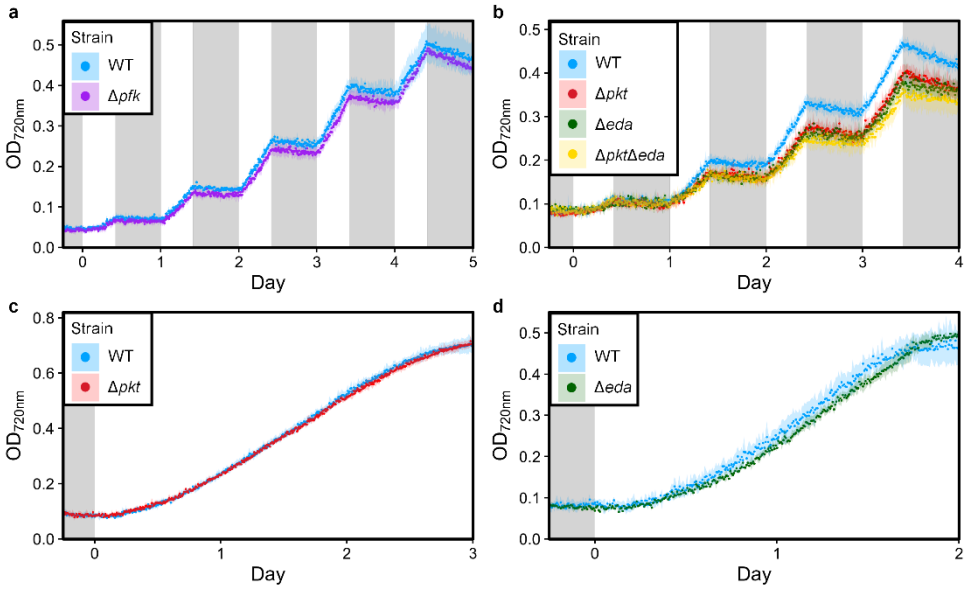

Figure 2. Phosphoketolase and KDPG aldolase contribute to robust diel growth. a, *S. elongatus* wild type (WT) and the phosphofructokinase mutant (Δ*pfk*) showed similar diel growth during the 10h/14h light/dark cycles, with statistically equal ($p = 0.478$) terminal OD_{720nm}. **b,** Diel growth of the phosphoketolase mutant (Δ*pkt*), the KDPG aldolase mutant (Δ*eda*), and the *pkt*/*eda* double mutant (Δ*pkt*Δ*eda*) during the 10h/14h light/dark cycles, showing significantly lower ($p <$

140 0.05) OD_{720nm} than WT by the end of the final light period. **c,** Similar growth of *S. elongatus* WT
141 and the Δ*pkt* mutant under the continuous light ($p = 0.774$). **d,** Similar growth of *S. elongatus* WT
142 and the Δ*eda* mutant under the continuous light ($p = 0.627$). Light intensity during the light period
143 was set to 100 μmol/m^2/s. Dotted line and shade represent the OD_{720nm} mean and standard
144 deviation, respectively. Grey shading represents the dark period of diel cycles as well as the 6 h of
145 initial dark adaptation to reset the circadian clock.
146

147 **Phosphoketolase and KDPG aldolase mutants have high respiration rates in the dark**

148 To dissect the contribution of phosphoketolase and KDPG aldolase in dark respiration, we
149 compared the respiration rates of Δ*pkt*, Δ*eda*, and Δ*pkt/eda* mutants with the wild type in the dark.
150 Following a few 10h/14h light/dark cycles, cells were collected in the next dark period to measure
151 respiration rates using a Clark-type oxygen electrode (Supplementary Fig. 3). For all four strains,
152 respiration rates increased quickly when cells entered darkness and remained high in the first half
153 of the night (Fig. 3a). The respiration rates of wild type cells decreased to base levels in the second
154 half of the night, corroborating with the minimal glycogen degradation activities during the latter
155 period of the dark (Fig. 1b and Fig. 3a). Remarkably, all mutants exhibited higher respiration rates
156 than the wild type throughout the latter part of the night. Notably, the Δ*pkt/eda* mutant was not
157 able to return to the base level respiration even at the end of the dark period (Fig. 3a).

158 When cells resumed growth in the light, the overall photosynthetic rates were similar among
159 all strains, measured by oxygen evolution rates both in one hour and eight hours in the light (Fig.
160 3b and Supplementary Fig. 4). This result shows that photosynthetic energy production is
161 unaffected in these mutants. Moreover, all strains demonstrated higher photosynthetic efficiency
162 in the latter part of the light period (Fig. 3b). However, all three mutants seem to have higher day
163 respiration rates compared to the wild type (Fig. 3b), indicating extended higher carbon loss in the
164 light due to disrupted cell metabolism. These results show the importance of phosphoketolase and
165 KDPG aldolase in dark respiration and carbon conservation during diel light/dark growth in
166 cyanobacteria.

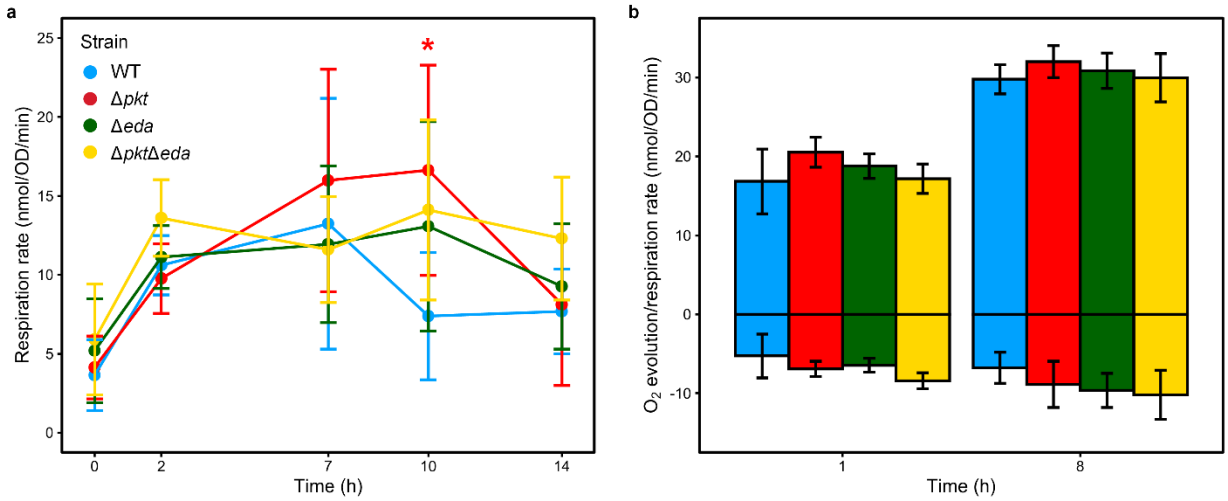

Figure 3. Phosphoketolase and KDPG aldolase mutants exhibit high respiration rates during diel growth cycles. a, Dark respiration rates in the *S. elongatus* wild type, Δ*pkt*, Δ*eda*, and Δ*pkt/eda* mutants. Cells were collected in the fourth dark period under the 10h/14h light/dark cycle growth. The red asterisk indicates a significantly higher ($p < 0.05$) respiration rate in Δ*pkt* than in the wild type at 10 h of the dark period. **b,** Oxygen evolution rates corrected by respiration (positive values) and separately daytime respiration rates (negative values) in the *S. elongatus* wild type, Δ*pkt*, Δ*eda*, and Δ*pkt/eda* mutants when cells resume growth in the light period of the diel growth cycle. Oxygen evolution rates were measured at 1 h and 8 h in the light period. Error bars represent standard deviation.

KDPG aldolase rather than the ED pathway participates in dark respiration

In the cyanobacterium *Synechocystis* sp. PCC 6803, the ED pathway was suggested to support cell growth under both mixotrophic conditions in continuous light and autotrophic light/dark growth conditions[17]. Two key enzymes of the ED pathway are the 6-phosphogluconate (6PG) dehydratase (6PGDH) and the KDPG aldolase. However, no genuine 6PGDH gene has been annotated in the *S. elongatus* genome, and rarely exists in other cyanobacteria[18]. Previous research suggests that dihydroxy acid dehydratase (DHAD) (*ilvD*) in amino acid metabolism could serve as an alternative enzyme for the dehydratase activity in the ED pathway in cyanobacteria[17]. To

examine this possibility, we purified the *S. elongatus* DHAD enzyme (*ilvD*) and tested its activity toward the ED pathway intermediate 6PG. Although *S. elongatus* DHAD shares a similar predicted structure to the genuine 6PGDH of other bacteria (Supplementary Fig. 5), it showed no 6PG dehydratase activity and instead displayed strong activity toward its native substrate 2,3-dihydroxyisovalerate (Fig. 4a and Supplementary Fig. 6). These results suggest that DHAD is not an alternative enzyme for the ED pathway in *S. elongatus*. To examine whether an alternative enzyme could serve as 6PG dehydratase in *S. elongatus*, we conducted *in vitro* 6PGDH enzyme assay by supplementing 6PG to cell lysates of both light and dark incubated cells. However, KDPG, the product of 6PG dehydration, was not detected or below the detection limit in these cell lysates (Fig. 4b). These results strongly suggest that the ED pathway is incomplete in *S. elongatus*.

We further tested the activity of purified KDPG aldolase from *S. elongatus.* The result showed that *S. elongatus* KDPG aldolase can catalyze the conversion of KDPG to glyceraldehyde 3-phosphate (G3P) and pyruvate (Fig. 4c). With an incomplete ED pathway in *S. elongatus*, it is likely that KDPG aldolase contributes to respiration through alternative activities. KDPG aldolase was reported to potentially catalyze several chemical reactions, one of which is oxaloacetate decarboxylation[19]. We thus tested whether *S. elongatus* KDPG aldolase can act on oxaloacetate. The *in vitro* assay showed that KDPG aldolase has decarboxylation activity on oxaloacetate to form pyruvate and CO_2 (Fig. 4c), suggesting its potential involvement in respiration through this reaction in *S. elongatus*. Furthermore, the kinetics experiment showed that KDPG aldolase has a relatively low *K*m of 0.473 mM toward oxaloacetate (Fig. 4d). Together, these results show that the ED pathway is incomplete in *S. elongatus* with the KDPG aldolase potentially participating in respiration through its oxaloacetate decarboxylation activity.

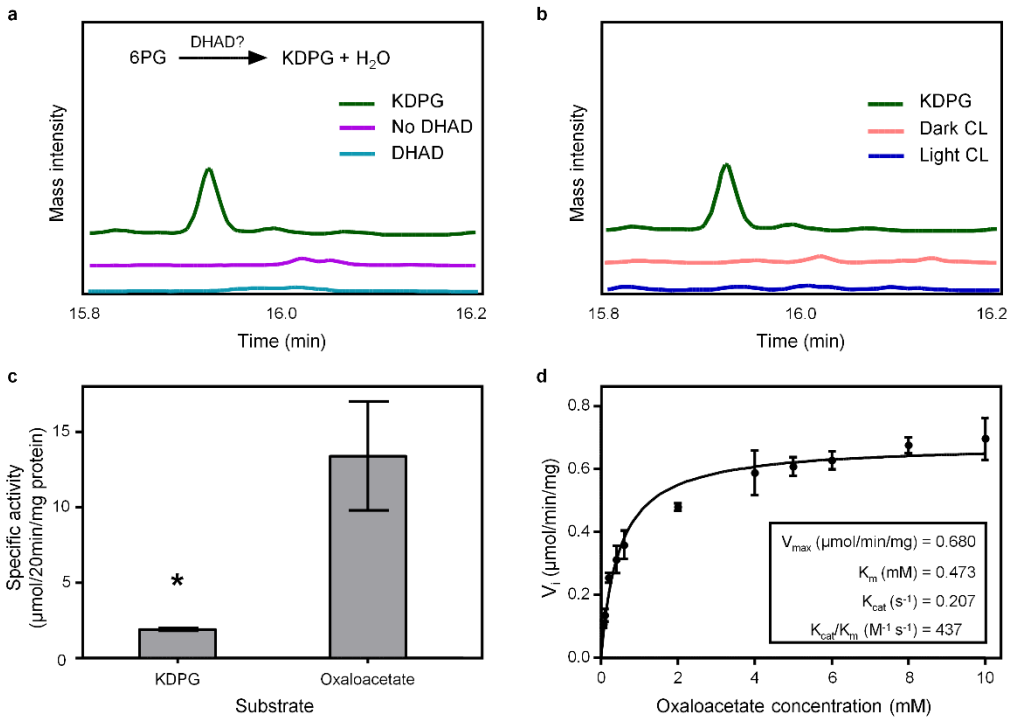

Figure 4. The ED pathway is incomplete in *S. elongatus*. 6PG dehydratase activity was monitored by the conversion of 6PG to KDGP as detected by GC-MS, with the retention time of the KDPG standard (green) displayed in **a** and **b**. **a,** *S. elongatus* DHAD displays no apparent 6PG dehydratase activity. No KDPG was detected when purified DHAD was supplemented to the 6PG dehydratase enzyme assay (cyan). Purple line shows the no enzyme control. **b,** 6PG dehydratase activity is not detected in the lysate of light or dark incubated cells. **c,** *S. elongatus* KDPG aldolase shows both KDPG cleavage activity and oxaloacetate decarboxylation activity. The asterisk indicates a significantly lower ($p < 0.05$) activity on KDPG than on oxaloacetate. **d,** Enzyme kinetics of the KDPG aldolase on the substrate oxaloacetate.

Phosphoketolase and KDPG aldolase mutants have disturbed cell metabolism in the dark

To better understand how phosphoketolase and KDPG aldolase contribute to dark respiration, we conducted a comparative metabolomics study on *S. elongatus* wild type, Δ*pkt*, and Δ*eda* mutants grown under the 10h/14h light/dark cycle. Following a few cycles of light/dark growth, cells were collected in four different time points in the third dark period (Supplementary Fig. 7).

226 Glycogen levels and degradation trends were similar among all three strains (Fig. 5a), indicating
227 enough glycogen was synthesized in the light period even with the disruption of phosphoketolase
228 or KDPG aldolase gene in the mutants.

229 The Δ*pkt* and Δ*eda* mutants have disturbed cell metabolism compared to the wild type,
230 indicated by distinct metabolite profiles in these strains; in each strain, the metabolite profiles also
231 differ largely between the beginning of the night and latter periods of the night (Fig. 5b,
232 Supplementary Table 2). When looking at biomarkers that separate these strains, the Δ*pkt* mutant
233 has the highest correlation with several amino acids (tyrosine, aspartate, threonine, and lysine),
234 whereas the Δ*eda* mutant has the highest correlation with metabolites such as ribose-5-phosphate
235 (R5P), oxoproline, and trans-4-hydroxyproline. The wild type, on the other hand, has the highest
236 correlation scores with carbohydrates such as 2PG and 3PG (Supplementary Table 3).

237 Comparative metabolomics suggests that phosphoketolase contributes to cell maintenance in
238 the dark by generating several precursors for amino acid synthesis. Phosphoketolase can convert
239 xylulose-5-phosphate (X5P) to G3P and acetyl-phosphate (acetyl-P), the latter of which can be
240 further converted to acetyl-CoA by acetate kinase and acetyl-CoA synthetase. Acetyl-CoA is a key
241 precursor for amino acid synthesis. If phosphoketolase contributes to significant acetyl-CoA flux,
242 the lack of acetyl-P production by the Δ*pkt* mutant could result in a shortage of acetyl-CoA and
243 further affect its reaction with oxaloacetate for α-ketoglutarate (AKG) synthesis in the oxidative
244 branch of the TCA pathway. This could lead to a transiently increased flux toward oxaloacetate
245 and its downstream amino acids. Corroborating with this, we observed a surge of threonine in the
246 first two hours of the dark and a consistently higher level of lysine in the Δ*pkt* mutant compared
247 to the other two strains (Fig. 5c), both of which are derived from oxaloacetate. The lack of acetyl-
248 CoA synthesis from acetyl-P likely needs to be compensated for by pyruvate decarboxylation,
249 resulting in additional 3PG consumption for pyruvate generation. In support of this notion, we
250 observed a much lower level of 3PG in the Δ*pkt* mutant compared to the other two strains (Fig.
251 5c). In addition, there was also a large increase of alanine in the Δ*pkt* mutant in comparison to the
252 other two strains in the first two hours of the dark period (Fig. 5c), supporting the increased flux

253 toward its precursor pyruvate.

254 The metabolomics further supports the oxaloacetate decarboxylation activity of KDPG
255 aldolase. When KDPG aldolase activity is disrupted in the Δ*eda* mutant, oxaloacetate is likely to
256 accumulate, thus leading to an increase of its downstream metabolites. Corroborating with this,
257 the Δ*eda* mutant accumulated a higher level of succinate during the latter half of the dark in
258 comparison to the other two strains (Fig. 5c), suggesting succinate generation from oxaloacetate
259 in the reductive branch of the TCA pathway. Additionally, glutamate, the amino acid synthesized
260 from AKG, was accumulated in the Δ*eda* mutant but not in the wild type during the first half of
261 the dark (Fig. 5c), suggesting an increased flux from oxaloacetate to AKG through the oxidative
262 branch of the TCA pathway when KDPG aldolase is absent; in the Δ*pkt* mutant, however, the
263 glutamate level decreased throughout the dark period (Fig. 5c), potentially due to the shortage of
264 acetyl-CoA to react with oxaloacetate. These above results collectively show that phosphoketolase
265 and KDPG aldolase are important enzymes for cell maintenance in the dark by generating
266 precursors for amino acid synthesis.

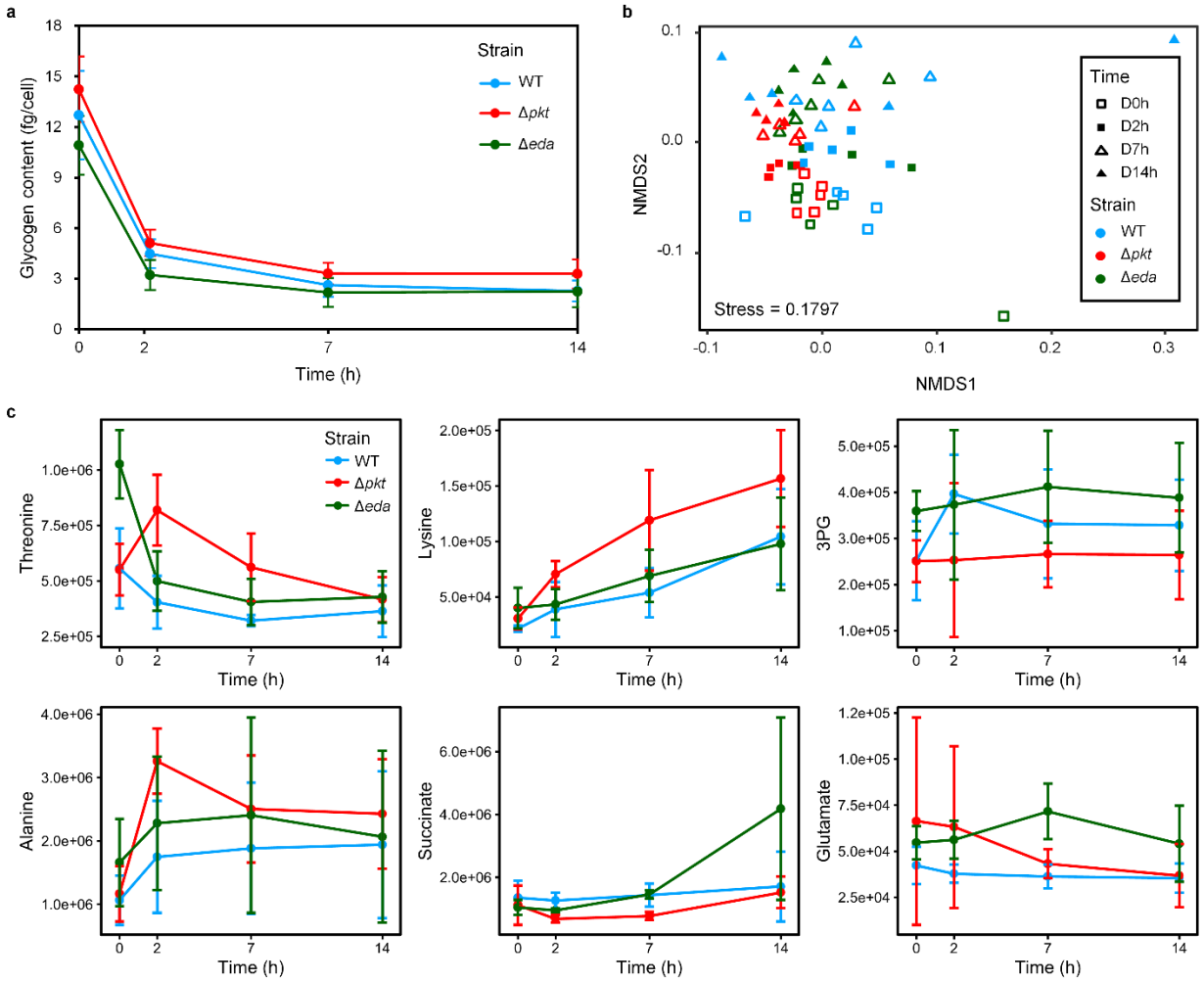

Figure 5. Phosphoketolase and KDPG aldolase mutants have disrupted amino acid synthesis in the dark. a, Glycogen degradation in the *S. elongatus* wild type, Δ*pkt*, and Δ*eda* mutants in the dark under 10h/14h light/dark cycle growth. **b,** Bray-Curtis distance matrix reflects the distinct metabolite profiles in the *S. elongatus* wild type, Δ*pkt*, and Δ*eda* mutants. **c,** Abundance changes of key intermediates in the dark in the *S. elongatus* wild type, Δ*pkt*, and Δ*eda* mutants.

Glycogen respires through an integrative metabolic network for cell maintenance and photosynthesis preparation in the dark

To gain an overview of these respiratory pathways in participating dark respiration, we conducted a time course proteomics on *S. elongatus* wild type under diel growth. The wild type was grown for three and a half cycles under 14h/10h light/dark cycles to obtain sufficient biomass,

279 followed by sample collection at various time points of dark and light periods in the next 24 hours.
280 In these proteomic samples, enzymes related to glycogen degradation (GlgP, glycogen
281 phosphorylase) and the OPP pathway (Zwf, G6P dehydrogenase) were found in greater abundance
282 in the dark than the light period (Fig. 6). This finding is consistent with the understanding of
283 glycogen as the major carbon and energy source for dark respiration[20].

284 Next, phosphoketolase metabolism likely connects the OPP pathway with the downstream
285 EMP pathway (Fig. 6). Phosphoketolase directly converts C_5 carbons derived from the OPP
286 pathway, involving less enzymatic steps for G3P generation compared to the non-oxidative pentose
287 phosphate (NOPP) pathway. In support of this notion, we found phosphoketolase and acetyl-CoA
288 synthetase (AcsA) have consistently high abundance throughout the diel cycle (Fig. 6).

289 Furthermore, the downstream EMP pathway is involved in converging glycogen degradation
290 products into key precursor metabolites for amino acid synthesis, including 3PG and
291 phosphoenolpyruvate (PEP) (Fig. 6). G3P from the phosphoketolase reaction is first converted to
292 3PG in the downstream EMP pathway. Particularly, enzymes responsible for forming and
293 oxidizing 3PG in the EMP pathway show distinct trends. On the one hand, G3P dehydrogenase
294 (Gap1), the enzyme converting G3P to 1,3-bisphophoglycerate (BPG), increased in the first half
295 of the night (Fig. 6). On the other hand, phosphoglycerate mutase (Pgam) and enolase (Ena),
296 responsible for converting 3PG to 2-phosphoglycerate (2PG) and PEP, were relatively stable in the
297 dark (Fig. 6), potentially restricting 3PG conversion flux. The combined effort by these enzymes
298 supports the notion that a portion of 3PG from glycogen degradation is diverted to amino acid
299 synthesis (Fig. 6). Moreover, PEP synthase (Pps) increased to a significantly higher level in the
300 first half of the night and stayed high throughout the dark, followed by a quick decrease to the base
301 level in the next light period (Fig. 6), suggesting the conversion of pyruvate into PEP in the latter
302 half of the night.

303 KDPG aldolase rather than pyruvate kinase is likely involved in pyruvate generation in the
304 latter half of the night. We found that PEP carboxylase (Ppc), responsible for converting PEP to
305 oxaloacetate, increased continuously in the dark (Fig. 6a). This was further supported by the

306 pyruvate kinase (Pyk) changes in the dark, with its level increasing during the first half of the night
307 and decreasing afterwards (Fig. 6). To synthesize amino acids derived from pyruvate when
308 pyruvate kinase levels are low in the latter half of the night, pyruvate generation could be
309 supplemented by the oxaloacetate decarboxylation activity of KDPG aldolase. This helps explain
310 the decreased biomass accumulation in the Δ*eda* mutant relative to the wild type under diel
311 light/dark cycles (Fig. 2). However, we found no KDPG aldolase peptides in the wild type
312 proteomic samples. It is likely that the KDPG aldolase enzyme kinetics could partially compensate
313 for its low abundance during diel light/dark growth.

314 Collectively, the proteomics coupled with diel growth and biochemistry assays reveal an
315 integrative respiratory pathway for dark respiration, where glycogen is first degraded to produce
316 NADPH and C_5 carbons in the OPP pathway, followed by C_5 conversion to G3P and acetyl-P by
317 the phosphoketolase metabolism. The intermediates G3P and acetyl-P further participate in the
318 EMP and acetyl-P conversion metabolisms to generate precursor metabolites for amino acid
319 synthesis, including 3PG, PEP, oxaloacetate, acetyl-CoA, and pyruvate. Meanwhile, KDPG
320 aldolase potentially contributes to additional pyruvate generation from oxaloacetate (Fig. 6). The
321 proposed route thus serves two purposes by optimizing carbon and energy allocation used for
322 amino acid synthesis in cell maintenance and helping 3PG accumulation for carbon fixation
323 reactions upon light exposure.

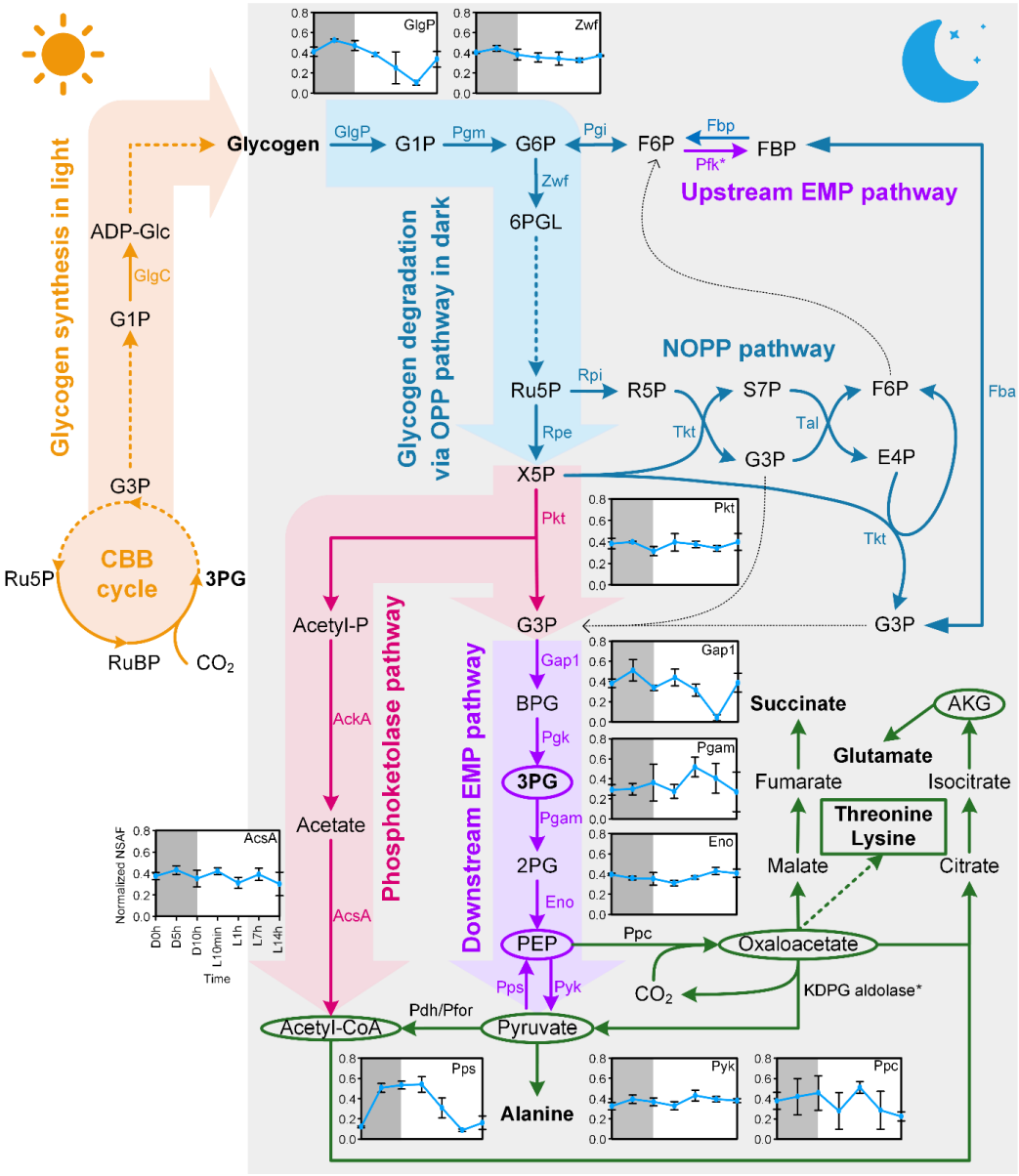

Figure 6. An integrative respiratory network in the dark. Metabolites labeled with oval shapes indicate precursor pools for amino acid synthesis, and those with bold texts are illustrated in Fig. 5. Inserted line plots show dynamic changes of key enzymes involved in dark respiration during a 14h/10h light/dark cycle in the *S. elongatus* wild type. The circle and error bar resent the mean and standard deviation, respectively. Grey shading indicates the dark period of the diel cycle. Asterisks at Pfk and KDPG aldolase indicate that these two enzymes were not detectable in the proteomic samples.

Discussion

Respiration in the dark contributes to significant carbon loss and lowers the overall photosynthetic carbon yield in cyanobacteria and other photosynthetic organisms. However, not much is understood about how these organisms achieve optimal carbon and energy allocation for dark respiration and its role in supporting photosynthesis. Here we show that in *S. elongatus*, cells form an integrative respiratory network in the dark to support optimal cell maintenance and prepare for carbon fixation reactions upon light exposure. This orchestrated respiratory network involves the OPP pathway, the phosphoketolase metabolism, and the EMP pathway. We further show that the ED pathway is incomplete in *S. elongatus*, with the KDPG aldolase participating in dark respiration through an alternative activity on oxaloacetate.

Phosphoketolase is an important glycolytic enzyme in many bacteria but its role in cyanobacteria is still under debate[21]. Previously, phosphoketolase was shown to carry significant carbon flux under mixotrophic conditions in an engineered *Synechocystis* sp. PCC 6803 strain[22]. We show here that phosphoketolase metabolism is critical for dark respiration under light/dark diel growth in the obligate photoautotrophic *S. elongatus*. When cyanobacteria enter the dark, phosphoketolase reaction connects the OPP pathway with amino acid synthesis for cell maintenance in the dark (Fig. 6). A recent bioinformatics study analyzed the possible co-occurrence of four glycolytic pathways (EMP, ED, OPP, and phosphoketolase) in cyanobacteria and found that the phosphoketolase and OPP pathways had the highest co-occurrence probability of 84.8% compared to all other combinations[18], supporting the OPP-phosphoketolase route in the dark during cyanobacterial diel light/dark growth. In addition, phosphoketolase exists in other eukaryotes such as diatom (Supplementary Fig. 8), suggesting its role in broader photosynthetic organisms.

In our study, phosphoketolase was found at consistent levels in the wild type throughout a diel light/dark cycle (Fig. 6). If phosphoketolase is allowed to work under light, its activity toward either X5P or F6P would likely lead to unstable CBB cycle reactions and retarded growth[23]. A previous research showed that phosphoketolase has much higher activities on X5P than F6P in *S.*

360 *elongatus*, with both activities significantly inhibited by ATP[24]. This helps explain the similar
361 growth of the wild type and the Δ*pkt* mutant under continuous light (Fig. 2c), suggesting that
362 phosphoketolase activity is likely regulated mainly at the allosteric rather than transcriptional level
363 during diel growth. When ATP level lowers upon cell entering the dark[25], phosphoketolase can be
364 activated to catalyze X5P cleavage. A more recent report confirmed the allosteric regulation of
365 phosphoketolase by ATP, and further showed an increased phosphoketolase activity during light-
366 dark transitions to brake on the CBB cycle and switch cell metabolism into respiration[26].

367 Phosphoketolase metabolism further contributes to robust diel cell growth by minimizing
368 carbon loss in the dark. When phosphoketolase was deleted in the Δ*pkt* mutant, less robust growth
369 was observed under the 10h/14h light/dark cycles (Fig. 2 and Supplementary Fig. 9). Without
370 phosphoketolase, the Δ*pkt* mutant will likely obtain G3P through transketolase reactions in the
371 NOPP pathway by converting R5P and X5P into G3P and sedoheptulose-7-phosphate (S7P) or
372 converting erythrose-4-phosphate (E4P) and X5P into G3P and fructose 6-phosphate (F6P) (Fig.
373 6). The siphoning of G3P from NOPP leads to imbalanced carbon pools, likely resulting in S7P
374 and F6P accumulation. Although we did not detect these phosphorylated sugars in our
375 metabolomics, this hypothesis is supported by findings in a previous study where *S. elongatus*
376 Δ*pkt* mutant was grown to high density and placed in darkness. In this study, significantly higher
377 levels of S7P and hexose-6P were found in the Δ*pkt* mutant than the wild type cells in the dark[24].
378 In addition, significantly lower amount of 3PG, PEP, and acetyl-CoA were found in the Δ*pkt*
379 mutant than the wild type, whereas pyruvate was accumulated to a higher level in the Δ*pkt* mutant[24].
380 In our study, the Δ*pkt* mutant also had much lower 3PG levels at the end of the dark period than
381 both wild type and the Δ*eda* mutant (Fig. 5b). This is likely due to increased consumption of 3PG
382 in the Δ*pkt* mutant to generate pyruvate and acetyl-CoA in the downstream EMP pathway, which
383 would lead to higher carbon loss in the pyruvate decarboxylase reaction. This suggests
384 phosphoketolase metabolism contributes to significant flux for acetyl-CoA generation from acetyl-
385 P, explaining the observed acetyl-CoA accumulation in the wild type in the previous study[24].
386 However, this hypothesis needs to be further tested by verifying activities of the two enzymes

387 involved in converting acetyl-P to acetyl-CoA in the dark.

388 The integrative OPP-Phosphoketolase-EMP route funnels glycogen degradation products into
389 several key precursor metabolites for amino acid synthesis, including pyruvate, PEP, and
390 oxaloacetate. Both PEP synthase and PEP carboxylase levels increased significantly in the first
391 half of the night and stayed high throughout the dark (Fig. 6), indicating increased activities to
392 synthesize oxaloacetate in the dark. On the other hand, pyruvate kinase levels peaked in the middle
393 of the night and decreased afterwards (Fig. 6), suggesting a limited flux to synthesize pyruvate
394 from PEP in the second half of the night. To this end, KDPG aldolase enzyme is likely important
395 during the latter half of the night to synthesize pyruvate from oxaloacetate (Fig. 6). This hypothesis
396 is supported by the observation that a significantly higher amount of succinate was accumulated
397 in the Δ*eda* mutant in the second half of the night (Fig. 5c). The deletion of the KDPG aldolase
398 enzyme could have led to the accumulation of oxaloacetate and its conversion to succinate in the
399 reductive branch of the TCA pathway[27].

400 KDPG aldolase contributes greatly to the robust diel growth in *S. elongatus*, as shown by
401 much lower biomass accumulation in the Δ*eda* mutant compared to the wild type under light/dark
402 cycles (Fig. 2). A similar retarded growth was observed in the Δ*eda* mutant of *Synechocystis* sp.
403 PCC6803 when cells grew photoautotrophically under light/dark cycles[17]. This previous study
404 attributed the growth defect to the absence of the ED pathway. However, no active 6PGDH activity
405 or KDPG metabolite were detected in *S. elongatus* (Fig. 4). In addition, the *in vitro* enzyme assay
406 of KDPG aldolase shows a much higher activity toward oxaloacetate than KDPG (Fig. 4c). Our
407 results thus strongly support that the ED pathway is incomplete in *S. elongatus* with the KDPG
408 aldolase participating in respiration through its alternative decarboxylation activity. This is also
409 consistent with the findings that the KDPG aldolase is much more prevalent than 6PGDH in
410 cyanobacteria[18].

411 The importance of the KDPG aldolase enzyme in dark respiration surrounds the oxaloacetate
412 metabolism. Oxaloacetate connects the downstream EMP pathway with the TCA pathway, which
413 is responsible for generating AKG and pyruvate for amino acid synthesis (Fig. 6). The proteomics

414 suggests that KDPG aldolase could supplement for pyruvate generation in the latter half of the
415 night when pyruvate kinase levels are decreasing (Fig. 6), supporting dark respiration and
416 preparing for carbon fixation reactions upon photoinduction. The enzyme kinetics shows the *K*m
417 of 0.473 mM toward oxaloacetate but a relatively low *k*cat/*K*m of 437 M^{-1} s^{-1} (Fig. 4d). It is possible
418 that the recombinant KDPG aldolase does not fully reflect its native enzyme activity due to the
419 addition of His-tag. In addition, the native KDPG aldolase was found to be trimers in many
420 bacteria[28], which could affect its activity if not assembled correctly *in vitro*.

421 Overall, our study reveals how dark respiration contributes to photosynthetic carbon yield,
422 and further shows the importance of phosphoketolase and KDPG aldolase in supporting robust
423 diel light/dark growth in cyanobacteria. Without these two enzymes participating in dark
424 respiration, the rewired cell metabolism results in disturbed cell metabolism and high respiration
425 in the dark, particularly in the latter half of the night (Fig. 3 and Fig. 5). Moreover, the disrupted
426 cell metabolism extends its impact on daytime metabolism as well, resulting in higher carbon loss
427 and lower biomass yield under diel light/dark cycles in cyanobacteria (Fig. 2 and Fig. 3). Further
428 validation of the proposed roles in algae and plants could help understand the prevalence of these
429 enzymes in phylogenetically diverse phototrophic taxa, and how compartmentation in eukaryotes
430 changes the role of glycolytic routes in dark respiration and photosynthesis robustness.

431

432 **Methods**

433 **Strain construction**

434 Plasmids required for generating mutant strains were prepared using HiFi DNA assembly
435 (NEB, USA) and then transformed into *S. elongatus* wild type. The DNA fragments for
436 construction of the plasmids were obtained through either high-fidelity amplification using Q5
437 DNA Polymerase (NEB, USA) or restriction enzyme digestion. The strains and plasmids
438 information can be found in Supplemental Fig. 1 and Supplemental Table 1. The mutant strains
439 were confirmed by segregation PCR.

440 **Growth characterizations**

441 The wild type and mutant strains of *S. elongatus* were grown in BG11 medium supplemented
442 with 20 mM $NaHCO_3$ and 10 mM N-[Tris(hydroxymethyl)methyl]-2-aminoethanesulfonic acid
443 (TES, pH 7.8) at 30 °C under 100 μmol/m^2/s (otherwise specified) cool white LED illumination
444 or different diel cycles in the Multi-Cultivator MC 1000-OD (Photon Systems Instruments, Czech
445 Republic). Growth was directly monitored by recording the absorbance at 720 nm at 10 min
446 intervals using the built-in optical density sensor. For the mutant strains, proper antibiotics were
447 supplemented to the growth medium. Cultures for proteomic and metabolomic analyses were
448 grown in the same medium and light conditions as described above.

449 **Oxygen evolution and respiration rate determination**

450 Four biological replicates of *S. elongatus* wild type, Δ*pkt*, Δ*eda*, and Δ*pkt*Δ*eda* mutant strains
451 were sampled at 0h, 2h, 7h, 10h, and 14h of the dark period of the fourth 10h/14h light/dark cycle,
452 and at 1h and 8h of the following light period. For each sample, 2 mL of culture was collected for
453 respiration and oxygen evolution rate determination using the Oxytherm+P system (Hansatech
454 Instruments) at 30°C. The respiration rates of the dark-period samples were normalized by OD_{720nm}
455 (recorded by the PSI multi-cultivator). The oxygen evolution rates of the light-period samples were
456 measured under saturated light, corrected by dark respiration rates, and normalized by either
457 OD_{720nm} or chlorophyll-a. The chlorophyll-a was extracted by 90% cold acetone supplemented
458 with 4 cycles of 45-sec bead beating (at 2400 rpm). OD_{665nm} and OD_{720nm} of the supernatant were
459 read by a GENESY 30 Visible Spectrophotometer (Thermo Scientific) to calculate the chlorophyll-
460 a concentration according to the equation: Chl_a [μg/ml] = 12.9447 (A665 − A720)[29].

461 **Derivatization and detection of KDPG and other metabolites by gas chromatography-mass**
462 **spectrometry (GC-MS)**

463 The samples and standards used in GC-MS analysis were prepared using the N-methyl
464 trifluoroacetamide (MSTFA) derivatization method. For derivatization reactions, 40 μL of 2%
465 methoxyamine hydrochloride (dissolved in pyridine) was added to freeze-dried samples, followed
466 by shaking at 37 °C for 2 h. After a brief spin, 70 μL of MSTFA with 1% trimethylchlorosilane
467 (TMCS) was added, followed by shaking at 37 °C for 30 min. After centrifugation at 17,000 g for

468 5 min, about 80 μL of the clear supernatant was transferred into a GC vial. KDPG standards
469 spanning from 11 to 176 pmol, supplemented with L-norvaline as the internal standard, were
470 prepared, dried, and derivatized in parallel with the samples to establish a calibration curve for
471 KDPG detection. The derivatized samples were run on a Thermo GC-MS equipment coupled with
472 the Zebron ZB-5MSplus column. The temperature program was set to 85 °C with an initial hold
473 for 2 min, followed by 10 °C/min of increase till 110 °C, 5 °C/min of increase till 230 °C, and
474 15 °C/min of increase till 320 °C, with a final hold for 2 min. The MS scan was set for the range
475 of 70-600 amu.

476 **Crude enzyme assays**

477 Crude enzyme assay was used to determine potential 6PG dehydratase activity by *S.*
478 *elongatus*. For crude protein extraction, *S. elongatus* wild type cells were grown in liquid BG11
479 medium until OD_{730nm} reached 2. After 6 hours of dark adaptation, 10 mL of each culture was
480 centrifuged at 8,000 g for 10 minutes at 4°C. The cell pellet was washed twice with 5 mL of cold
481 50 mM Tris-HCl buffer (pH 8) containing 1× Protease Inhibitor Cocktail, and finally resuspended
482 in 1000 μL of this buffer. The resuspended cells were lysed using 0.1 mm diameter silicone beads
483 in a bead beater for 15 cycles of 10 sec on and 2 min off on ice. The supernatant containing the
484 crude protein was separated by centrifugation at maximum speed for 10 minutes at 4°C. The
485 protein concentration in the supernatant was determined by Bradford assay.

486 The crude lysate reaction mix containing 50 mM Tris-HCl buffer, 100 mM NaCl and 100 μL
487 of the crude lysate was preincubated at 30 °C for 15 minutes. The reaction was initiated using 2.5
488 mM 6-phosphogluconic acid as the substrate. The reaction was incubated at 30°C for two hours in
489 light and dark respectively. Samples were analyzed for KDPG production using GC-MS.

490 **Recombinant enzyme purification and *in vitro* enzyme assays**

491 To check the activity of DHAD (*ilvD*) and KDPG aldolase (*eda*), the gene fragment was
492 amplified from the genome of *S. elongatus*, linked with the his-tag containing pET28A vector
493 using Gibson assembly, and transformed into *E. coli* BL21 competent cells. To extract the his-
494 tagged protein, 100 mL of the transformant cells were grown until OD_{600nm} reached ~0.5, when

495 0.1 M IPTG was added to induce the overexpression of the his-tagged protein. After 4 h of
496 induction, the culture was centrifugated at 6,000 rpm and 4 °C for 10 min. The cells were washed
497 twice with 5 mL of cold 100 mM Tris-HCl buffer (pH 8), resuspended in 1 mL of the buffer
498 supplemented with 1× Protease Inhibitor Cocktail, and then lysed by 0.1 mm diameter silicone
499 beads in a bead beater for 15 cycles of 10 sec on and 30 sec off on ice. The lysate was collected
500 after centrifugation at maximum speed for 10 minutes at 4 °C. The targeted his-tagged protein was
501 purified using the NEB Express Ni Spin Columns (catalog no. S1427) following the
502 manufacturer's protocol and confirmed by SDS-PAGE (Supplementary Fig. 10).

503 To test KDPG aldolase activities, the his-tagged KDPG aldolase enzyme was coupled with
504 Lactate Dehydrogenase (LDH): NADH assay to detect pyruvate generation using KDPG or
505 oxaloacetate as the substrate. The reaction mixture contained 100 mM Tris-buffer (pH 8), 150 mM
506 NaCl, 2 mM NADH, 6 units of LDH, 5 μL of purified KDPG aldolase, and 2 mM of the required
507 substrate. The rection mixture without substrate was preincubated for 15 minutes at 30°C and later
508 2 mM substrate was added to initiate the reaction. The reactions without substrate and without
509 enzyme were prepared separately as controls. The initial absorbance (OD_{340nm}) was read in the
510 microplate reader and allowed to incubate until a drop in the absorbance was observed. The
511 absorbance at 340 nm was read every 10 minutes to generate NADH oxidation curve over time.

512 To determine whether DHAD can function as 6PGDH to catalyze the conversion of 6PG to
513 KDPG, the reaction mixture containing 50 mM Tris HCl (pH 7.8), 150 mM NaCl, 1 mM $MgCl_2$
514 and 10 μL purified DHAD was preincubated for 15 minutes. The reaction was initiated using 2.5
515 mM 6PG as substrate and was incubated at 30 °C for 1 h. The reaction was then anaylzed using
516 GC-MS for production of KDPG as the product. The native DHAD activity for conversion of 2,3-
517 dihydroxyisovalerate to ketoisovalerate was used as positive control. For this activity, the reaction
518 was initiated using 2,3-dihydroxyisovalerate as the substrate and production of ketoisovalerate was
519 analyzed using GC-MS.

520 **Determination of KDPG aldolase kinetics on oxaloacetate**

The oxaloacetate decarboxylating activity of KDPG aldolase was measured at different concentrations to generate the Michaelis-Menten curve for the calculation of K_m and V_{max} values. The reaction mix containing 100 mM Tris buffer (pH 8), 150 mM NaCl, 2 mM NADH, 6 units of LDH and 5 μL of purified KDPG aldolase was preincubated for 15 minutes at 30 °C. The reaction was initiated using a range of substrate concentrations (0.075-10 mM) and was allowed to incubate at 30°C for 20 minutes. The drop in OD_{340nm} was normalized to the no-enzyme control due to spontaneous decarboxylation of oxaloacetate. The experimental data for the initial slope was used for kinetics measurements and was fitted through the Michaelis-Menten equation using Graphpad software for calculation of V_{max}, K_m, and k_{cat} values.

Acknowledgements

We thank Julie Maupin-Furlow for insightful suggestions and careful reading of the manuscript. We thank Rachael Morgan-Kiss for providing access to the PSI multi-cultivator and the Center for Bioinformatics and Functional Genomics at Miami University for providing access to several equipment used in this study. This work was supported by the National Science Foundation grant number 2042182. X.W. would like to acknowledge support from both University of Florida and Miami University.

Author contributions

X.W. conceived the project. N.X., and K.R. performed the genetics, proteomics, and growth physiology experiments. C.S. performed the enzyme kinetics experiment. N.X. and X.W. wrote the manuscript with edits from C.S.

Competing interests

The authors declare no competing interests.

Data availability

All data are presented in the main text and supplemental materials. Proteomics data has been deposited into the public database MassIVE repository and ProteomeXchange Consortium.

References

1 Flombaum, P. *et al.* Present and future global distributions of the marine Cyanobacteria *Prochlorococcus* and *Synechococcus*. *Proc. Natl. Acad. Sci. U. S. A.* **110**, 9824-9829 (2013). https://doi.org/doi:10.1073/pnas.1307701110

2 Field, C. B., Behrenfeld, M. J., Randerson, J. T. & Falkowski, P. Primary production of the biosphere: integrating terrestrial and oceanic components. *Science* **281**, 237-240 (1998). https://doi.org/doi:10.1126/science.281.5374.237

3 Welkie, D. G. *et al.* A hard day's night: Cyanobacteria in diel cycles. *Trends Microbiol.* (2018).

4 Zhu, X.-G., Long, S. P. & Ort, D. R. What is the maximum efficiency with which photosynthesis can convert solar energy into biomass? *Curr. Opin. Biotechnol.* **19**, 153-159 (2008). https://doi.org/https://doi.org/10.1016/j.copbio.2008.02.004

5 Hanson, A. D., Millar, A. H., Nikoloski, Z. & Way, D. A. Focus on respiration. *Plant Physiol.* **191**, 2067-2069 (2023). https://doi.org/10.1093/plphys/kiad041

6 Amthor, J. S. *et al.* Engineering strategies to boost crop productivity by cutting respiratory carbon loss. *Plant Cell* **31**, 297-314 (2019). https://doi.org/10.1105/tpc.18.00743

7 Munson-McGee, J. H. *et al.* Decoupling of respiration rates and abundance in marine prokaryoplankton. *Nature* **612**, 764-770 (2022). https://doi.org/10.1038/s41586-022-05505-3

8 Smith, A. J. Modes of cyanobacterial carbon metabolism. *Annales de l'Institut Pasteur / Microbiologie* **134**, 93-113 (1983). https://doi.org/https://doi.org/10.1016/S0769-2609(83)80099-4

9 Lea-Smith, D. J., Bombelli, P., Vasudevan, R. & Howe, C. J. Photosynthetic, respiratory and extracellular electron transport pathways in cyanobacteria. *Biochim. Biophys. Acta Bioenerg.* **1857**, 247-255 (2016). https://doi.org/10.1016/j.bbabio.2015.10.007

10 Diamond, S. *et al.* Redox crisis underlies conditional light–dark lethality in cyanobacterial mutants that lack the circadian regulator, RpaA. *Proc. Natl. Acad. Sci. U. S. A.* **114**, E580-E589 (2017).

11 Ohbayashi, R. *et al.* DNA replication depends on photosynthetic electron transport in cyanobacteria. *FEMS Microbiology Letters* **344**, 138-144 (2013). https://doi.org/10.1111/1574-6968.12166

12 Watanabe, S. *et al.* Light-dependent and asynchronous replication of cyanobacterial multi-copy chromosomes. *Mol. Microbiol.* **83**, 856-865 (2012). https://doi.org/10.1111/j.1365-2958.2012.07971.x

13 Tamoi, M., Miyazaki, T., Fukamizo, T. & Shigeoka, S. The Calvin cycle in cyanobacteria is regulated by CP12 via the NAD(H)/NADP(H) ratio under light/dark conditions. *The Plant Journal* **42**, 504-513 (2005). https://doi.org/https://doi.org/10.1111/j.1365-313X.2005.02391.x

14 Shinde, S. *et al.* Glycogen metabolism supports photosynthesis start through the oxidative pentose phosphate pathway in cyanobacteria. *Plant Physiol.* **182**, 507-517 (2020).

15 Tanaka, K. *et al.* Dark accumulation of downstream glycolytic intermediates initiates robust photosynthesis in cyanobacteria. *Plant Physiol.* **191**, 2400-2413 (2022). https://doi.org/10.1093/plphys/kiac602

16 Welkie, D. G. *et al.* Genome-wide fitness assessment during diurnal growth reveals an expanded role of the cyanobacterial circadian clock protein KaiA. *Proceedings of the National Academy of Sciences* **115**, E7174-E7183 (2018). https://doi.org/doi:10.1073/pnas.1802940115

17 Chen, X. *et al.* The Entner-Doudoroff pathway is an overlooked glycolytic route in cyanobacteria and plants. *Proc. Natl. Acad. Sci. U. S. A.* **113**, 5441-5446 (2016). https://doi.org/10.1073/pnas.1521916113

18 Bachhar, A. & Jablonsky, J. Entner-Doudoroff pathway in *Synechocystis* PCC 6803: Proposed regulatory roles and enzyme multifunctionalities. *Front Microbiol.* **13**, 967545 (2022). https://doi.org/10.3389/fmicb.2022.967545

19 Mavridis, I. M. & Tulinsky, A. The folding and quaternary structure of trimeric 2-keto-3-deoxy-6-phosphogluconic aldolase at 3.5-A resolution. *Biochemistry* **15**, 4410-4417 (1976). https://doi.org/10.1021/bi00665a010

20 Smith, A. Modes of cyanobacterial carbon metabolism. *Ann. Inst. Pasteur Microbiol.* **134**, 93-113 (1983).

21 Årsköld, E. *et al.* Phosphoketolase pathway dominates in ATCC 55730 containing dual pathways for glycolysis. *J. Bacteriol.* **190**, 206-212 (2008). https://doi.org/10.1128/Jb.01227-07

22 Xiong, W. *et al.* Phosphoketolase pathway contributes to carbon metabolism in cyanobacteria. *Nat. Plants* **2**, 15187 (2015). https://doi.org/10.1038/nplants.2015.187

23 Yu, H., Li, X., Duchoud, F., Chuang, D. S. & Liao, J. C. Augmenting the Calvin–Benson–Bassham cycle by a synthetic malyl-CoA-glycerate carbon fixation pathway. *Nat. Commun.* **9**, 2008 (2018). https://doi.org/10.1038/s41467-018-04417-z

24 Chuang, D. S. W. & Liao, J. C. Role of cyanobacterial phosphoketolase in energy regulation and glucose secretion under dark anaerobic and osmotic stress conditions. *Metab. Eng.* **65**, 255-262 (2021). https://doi.org/10.1016/j.ymben.2020.12.004

25 Rust, M. J., Golden, S. S. & O'Shea, E. K. Light-Driven Changes in Energy Metabolism Directly Entrain the Cyanobacterial Circadian Oscillator. *Science* **331**, 220-223 (2011). https://doi.org/doi:10.1126/science.1197243

26 Lu, K.-J. *et al.* An ATP-sensitive phosphoketolase regulates carbon fixation in cyanobacteria. *Nat. Metab.* **5**, 1111-1126 (2023). https://doi.org/10.1038/s42255-023-00831-w

27 Iijima, H. *et al.* Four-carbon dicarboxylic acid production through the reductive branch of the open cyanobacterial tricarboxylic acid cycle in Synechocystis sp. PCC 6803. *Metab. Eng.* **65**, 88-98 (2021). https://doi.org/https://doi.org/10.1016/j.ymben.2021.03.007

28 Wymer, N. *et al.* Directed Evolution of a New Catalytic Site in 2-Keto-3-Deoxy-6-Phosphogluconate Aldolase from Escherichia coli. *Structure* **9**, 1-9 (2001). https://doi.org/https://doi.org/10.1016/S0969-2126(00)00555-4

29 Ritchie, R. J. Consistent Sets of Spectrophotometric Chlorophyll Equations for Acetone, Methanol and Ethanol Solvents. *Photosyn. Res.* **89**, 27-41 (2006). https://doi.org/10.1007/s11120-006-9065-9